

Isospectrally Patterned Aperiodic Lattices

Peter Schmelcher^{1,2,3,*}

¹Zentrum für Optische Quantentechnologien, Fachbereich Physik,
Universität Hamburg, Luruper Chaussee 149, 22761 Hamburg, Germany

²The Hamburg Centre for Ultrafast Imaging, Universität Hamburg,
Luruper Chaussee 149, 22761 Hamburg, Germany

³ITAMP, Center for Astrophysics | Harvard & Smithsonian Cambridge, Massachusetts 02138, USA

(Dated: June 27, 2024)

We design and explore patterned aperiodic lattices consisting of coupled isospectral cells that vary across the lattice. Each resulting band consists of three distinct energy domains with two mobility edges marking the transition from localized to delocalized states and vice versa. The characteristic localization length emerges due to a competition of the involved phase gradient and the coupling between the cells which allows us to understand the localization mechanism and its evolution. The fraction of localized versus delocalized eigenstates can be tuned by changing the gradient between the cells of the lattice. We outline the perspectives of investigation of this novel class of isospectrally patterned aperiodic lattices.

Introduction - Symmetries are ubiquitous in our description of quantum matter and represent a powerful means to analyze and classify its properties [1]. They define a unique starting-point for a subsequent deductive analytical or numerical study, a famous example being the theory of band structure which is based on Bloch's theorem due to crystalline translation invariance [2, 3]. The latter implies completely delocalized Bloch states. The absence of any symmetries in the case of disorder leads in one and two spatial dimensions to a spectrum of localized states [4, 5]. Quasicrystals with their aperiodic long-range order fall into the substantial gap between these two limiting cases [6–15]. They show fractal energy spectra, critical localization of eigenstates, and arrange in so-called quasibands [16–20]. The coexistence of localized and delocalized eigenstates in aperiodic systems can involve a so-called mobility edge which marks the transition energy separating the different classes of states [21] or can become manifest in an intermediate phase of interdispersed localized and delocalized states without mobility edge. The paradigm for exploring mixed localization-delocalization behaviour in one spatial dimension is the Aubry-André quasiperiodic model [22], whose modifications and generalizations have been extensively explored [23–39] in particular in recent years. They are crucial for our understanding of the occurrence of mobility edges and transport in quasiperiodic settings. Experimental platforms that lately discovered the localization-delocalization interplay and mobility edges inspired by the generalized Aubry-André setups include ultracold atoms [40–42] and cavity polaritons [43]. Also, mobility edges have been predicted [44] and experimentally observed [45] in microwave transition spectra in waveguides for one-dimensional random potentials in the presence of specific long-range correlations.

Quasicrystals do not possess global symmetries but a plethora of local symmetries [15, 46]. The impact of the presence of local symmetries in general settings, i.e. be-

yond the paradigm of quasicrystals, has been explored recently for both continuous and discrete one-dimensional systems [47–52]. Local symmetries allow to classify resonances in wave scattering [48, 49] and enhance the transfer efficiency in lattices [53]. Signatures of local symmetries have been observed experimentally in both lossy acoustic waveguides [54] and coupled photonic waveguide lattices [55]. A typical spectral feature in the presence of local symmetries is the localization of eigenstates on the corresponding local symmetry specific domains of a given lattice (see in particular [46]). The underlying mechanism of this steered localization behaviour has been identified [56] as the isospectrality of the isolated symmetry-related subdomains i.e. applying a reflection or translation operation does not alter the eigenvalues. As a consequence we obtain pairwise degenerate eigenvalues that split linearly with an increasing coupling strength of these symmetry-related subdomains. This is the key ingredient to the present work: we elevate these properties to a working principle that generates a new class of aperiodic lattices being composed of coupled isospectral cells, beyond the notion of local symmetries. At hand of a specific case, we demonstrate that these isospectrally patterned aperiodic lattices possess several mobility edges dividing each of the energy bands into three distinct branches. The branches of localized states are based on a characteristic localization length which results from the competition of the coupling and the (discrete) phase gradient relating different isospectral cells. We determine the behaviour of the fraction of (de-)localized states with varying phase gradient and coupling strength as well as system size.

Setup and Hamiltonian - According to [56] it is the isospectrality of symmetry-related (isolated) subdomains and the resulting pairwise degeneracy of eigenvalues which underlie the observed localization of eigenstates on locally symmetric domains. We therefore consider lattices that consist of isospectral cells $\mathbf{A}_m, m = 1, \dots, N$

coupled via off-diagonal blocks \mathbf{C}_m , which leads to the following Hamiltonian

$$\mathcal{H} = \sum_{m=1}^N (|m\rangle \langle m| \otimes \mathbf{A}_m) + \sum_{m=1}^{N-1} (|m+1\rangle \langle m| \otimes \mathbf{C}_m + h.c.) \quad (1)$$

reminiscent of the dividing of the state space into internal and external degrees of freedom. An immediate way of ensuring that the cells \mathbf{A}_m are isospectral is to choose them as orthogonal (or in general unitary) transformations of a diagonal matrix \mathbf{D} , i.e. we have $\mathbf{A}_m = \mathbf{O}_{\phi_m} \mathbf{D} \mathbf{O}_{\phi_m}^{-1}$, where ϕ_m indicates the (set of) angles specifying the transformation. In general $\mathbf{A}_m, \mathbf{C}_m$ are $K \times K$ finite sublattices residing on the diagonal and off-diagonal of the lattice. For the purpose of providing evidence of the richness of the spectral properties of \mathcal{H} , we specialize to the case $K = 2$, resulting in a single angle ϕ , and to $\mathbf{C} = \mathbf{C}_m = \frac{\epsilon}{2} (\sigma_x + i\sigma_y)$ using open boundary conditions for our aperiodic setup. The aperiodicity is implemented by our choice of the values ϕ_m : we choose an equidistant grid of angles centered around the value $\frac{\pi}{4}$. This choice is motivated by the fact that the eigenvectors of $\mathbf{A}_{\frac{\pi}{4}}$ are, independent of \mathbf{D} , maximally delocalized in the m -th cell, providing a distinct starting-point for the control of localization versus delocalization on the lattice consisting of many coupled cells. The complete angular (or phase) range covered by the lattice reads then $[\frac{\pi}{4} - \frac{L}{2}, \frac{\pi}{4} + \frac{L}{2}]$ with $L = \frac{\pi}{4} \cdot \frac{1}{L_f}$ where L_f is a scaling factor of the phase range of the lattice, and we have $\phi_m = \frac{\pi}{4} - \frac{L}{2} + \frac{m-1}{N-1}L$. Our lattice possesses, by construction, an inversion symmetry around its center $\phi = \frac{\pi}{4}$. We note, that for the limiting case $L_f \rightarrow \infty$ we obtain a periodic lattice with the unit-cell being $\mathbf{A}_{\frac{\pi}{4}}$ whereas for $L_f = 1.0$ the lattice covers the angular range $[\frac{\pi}{8}, \frac{3\pi}{8}]$. While we principally address the case of finite lattices in this work they can be arbitrarily large (see below). Our main focus will be on the weak to intermediate coupling regime $0 < \epsilon < 1$.

Phenomenology of the eigenvalue spectrum - We first analyze the eigenvalue spectrum belonging to the Hamiltonian \mathcal{H} in eq.(1) for an aperiodic lattice with several thousand sites and $L_f = 1.0$ for a coupling strength $\epsilon = 0.3$ and diagonal values $d_1 = 1, d_2 = 2$ of \mathbf{D} , as shown in Fig.1. We observe two bands separated by a band gap [57], our subsequent statements holding essentially for both bands. Each band can be divided into three distinct energy domains marked as A, B, C in Fig.1, which correspond to the lower, middle and upper energy domain of the lower band. Obviously, the energy eigenvalues with increasing degree of excitation show a prominent difference from the cosine-dispersion relation of the (monomer) periodic tight-binding case. In particular we witness close to the edges of the bands an approximately linear behaviour of the energies. To work this out in more detail,

the upper left inset in Fig.1 shows the spectrum of the eigenvalue spacing clearly exposing three domains with qualitatively different behaviour for each band. While the region A shows a linearly decreasing spacing, region B exhibits a highly nonlinear and nonmonotonic dependence, whereas region C displays a very peaked close to linear behaviour. The three domains can also be identified in the density of states shown as the lower right inset in Fig. 1. In region A we observe a high density of states which is even increasing within this domain and followed by a steep decline of the density of states in region B with partial recovery for higher energies, and finally, in region C, we observe an approximately linear decrease. This behaviour persists qualitatively with varying coupling strength, noting that the energy gap between the two bands closes for $\epsilon = 0.5$. With increasing value of L_f the covered phase interval shrinks and consequently the sizes of the domains A and B also shrink.

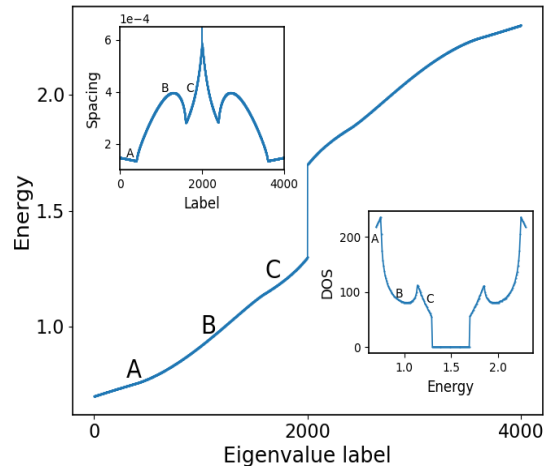


Figure 1. Main figure: energy eigenvalue spectrum of the equidistant ϕ lattice for $d_1 = 1, d_2 = 2, L_f = 1.0, \epsilon = 0.3, N_s = 4002$, where d_1, d_2 are the diagonal values of \mathbf{D} . Upper left inset: the corresponding energy level spacing. Lower right inset: the density of states for $N_s = 16002$. The labels A,B,C mark the three distinct energetical regimes of the band which reflect itself correspondingly in the level spacing and the density of states.

Eigenstate analysis: localization versus delocalization - We have identified above three distinct domains within each energy band which we analyze now in terms of the behaviour of their eigenstates. Fig.2 shows a greyscale eigenstate map, i.e. the magnitude of the eigenstate components, for the complete first band. The subfigures 2 (a,b,c) correspond to the domains A,B,C in the first energy band in Fig.1, respectively. We observe that in the domain A (Fig.2(a)) all eigenstates are localized and increasingly spread with increasing degree of excitation. In domain B the eigenstates are delocalized over the com-

plete lattice, and, finally, in domain C localization takes over again and the eigenstates become increasingly localized with increasing degree of excitation. This behaviour persists for varying coupling strength, in particular also for weak couplings, and for varying angular interval L (see below for quantitative statements) and is therefore of generic character. It repeats in the second upper band. We therefore encounter within each band two mobility edges marking the transition from localized to delocalized eigenstates.

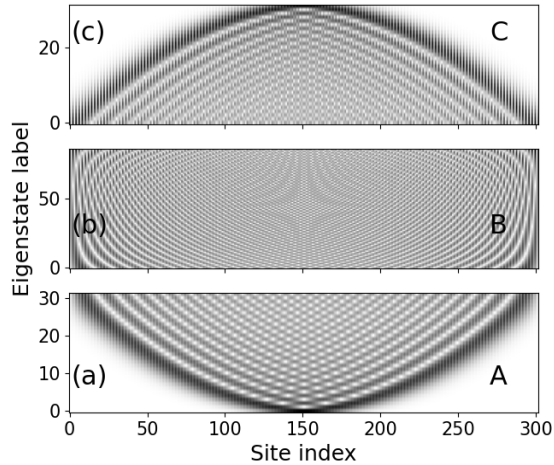


Figure 2. Grey scale eigenstate map showing the absolute values of all eigenstate components for the lower band of the spectrum of the lattice with $d_1 = 1, d_2 = 2, L_f = 1.0, \epsilon = 0.3, N_s = 302$. Note that the grey scale has been renormalized for each eigenstate row. The sequence of eigenstates is divided into three domains (a,b,c) according to the energy domains A,B,C of the lower band in Fig.1. Note that the counting of the eigenstate labels is reset to zero within each domain providing a total of 151 eigenstate profiles.

Let us inspect the eigenstate profiles in some more detail with the aim to understand the origin of our observed localization. Fig. 3 shows, for the same parameter values as in Fig. 2, the ground state as well as the first and tenth excited states in the first band, thereby observing the increasing spreading of the eigenstates. While our lattice consists of $N_s = 302$ sites, the ground state shows a localization length of the order of a 50 sites, whose origin and mechanism we shall analyze in the following. A closer inspection reveals that the envelope of the ground state is very well described by a Gaussian wave function. The fast oscillations from site to site can be attributed to the fact that $\mathbf{A}_{\frac{\pi}{4}}$ possesses (like all \mathbf{A}_m) the eigenvectors $(1, -1), (1, 1)$. Resultingly, a variational ansatz for the ground state wave function reads as follows

$$|\Psi\rangle = \mathcal{N} \sum_n \exp\left(-\alpha(n - n_0)^2\right) |n\rangle \otimes (1, -1) \quad (2)$$

where $\mathcal{N} = \frac{1}{\sqrt{2}} \left(\sum_n \exp\left(-2\alpha(n - n_0)^2\right) \right)^{-\frac{1}{2}}$ is the normalization constant and α is a variational parameter to be determined by minimizing the corresponding energy $E = \langle \Psi | \mathcal{H} | \Psi \rangle$. Evaluating this expectation value involves approximating the summations by continuous integrals and leads to the final result

$$E = \frac{1}{2}(d_1 + d_2) + \frac{1}{2}(d_1 - d_2) \exp\left(-\frac{1}{4\beta}\right) - \epsilon \exp\left(-\frac{\alpha}{2}\right) \quad (3)$$

where $\beta = \frac{8\alpha N^2}{\pi^2}$. Note that $\frac{\pi}{4NL_f}$ is the phase gradient across our lattice with $L_f = 1.0$ in the present case. The two competing second and third terms in the energy eq.(3) are due to the phase change across the cells on the diagonal and the off-diagonal coupling terms, respectively.

Varying α there exists a single minimum which amounts, for our specific case, to $\alpha_0 \approx 3.4 \cdot 10^{-3}$. The resulting energy agrees with the corresponding numerical value within one per mill. The full width half maximum for these analytical considerations is 29 sites as compared to the numerical value of approximately 43 sites. The observed localization behaviour therefore emerges in our aperiodic setup due to the competition in energy between the phase gradient among the isospectral cells and the coupling between the cells.

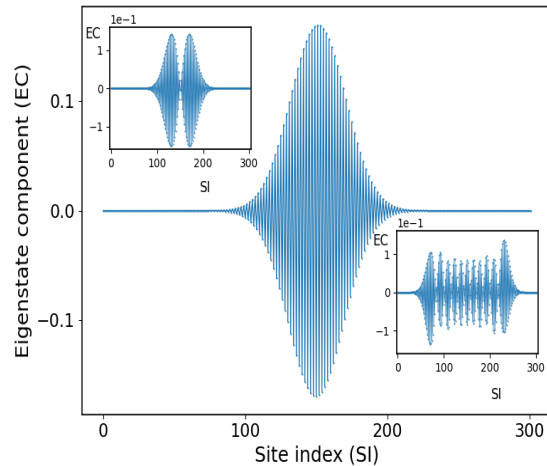


Figure 3. The localized ground (main figure) and first (top left inset) as well as tenth (bottom right inset) excited states of the first band in the domain A (see Figs.1,2).

The eigenstates at the upper band edge can be obtained in a similar manner. From the above analysis, the position of the mobility edge occurs at $n_{mob} \approx C \cdot \frac{N^2}{\sigma^2}$ where σ^2 is the variance of the Gaussian ground state and C being a constant of order one.

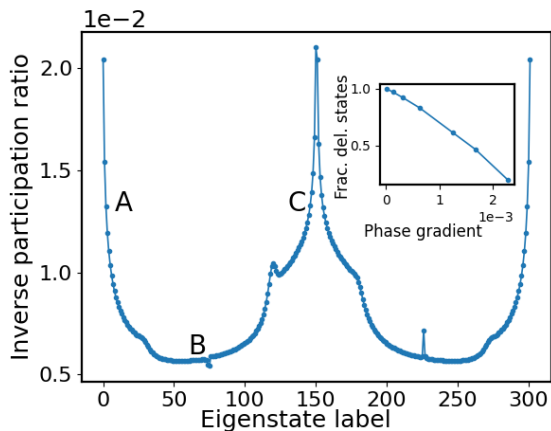


Figure 4. Main figure: The inverse participation ratio for all eigenstates across both bands. Parameters are the same as in Fig.2. Inset: The fraction of delocalized states with varying phase gradient for a fixed lattice size. Labels A,B,C correspond to the different energy domains (see Fig. 1).

To quantify our (de-)localization transition we determine the inverse participation ratio (IPR) for the complete spectrum of eigenstates, which is defined as $r = \sum_{i=1}^N |\psi_i|^4 \in [N^{-1}, 1]$. The maximal value for the IPR is one for an eigenvector localized on a single site of the chain and the minimal value $\frac{1}{N}$ is encountered for a state which is uniformly extended over the chain. As expected, the IPR is large in the domains A and C of localized states whereas it is smallest in the regime B of delocalized states where a plateau of low values is encountered. According to the increasing delocalization in regime A with increasing degree of excitation the IPR peaks strongly for the ground state and low excitations but then rapidly decays when approaching the regime B. The reverse happens at the upper edge of the first band. A central moment analysis allows equally to distinguish between the different domains A,B and C with all odd moments being zero.

Some discussion concerning the fraction of localized vs. delocalized states is in order. For a sufficiently large value of L_f practically all eigenstates are delocalized. With a decreasing value of L_f , i.e. an increasing phase gradient, we observe an approximately linear decrease of the fraction of delocalized states, see the inset of Fig.4. For e.g. $L_f = 1.0$ corresponding to a phase gradient of $1.2 \cdot 10^{-3}$ (for the above other parameter values) 40 % of the eigenstates become localized. The fraction of (de-)localized states is independent of the coupling strength ϵ . It is also independent of the lattice size which we have verified by varying it over three orders of magnitude in case we keep the total angular interval constant. Our observed localization delocalization transition is robust against disorder, both for the coupling and for the eigenvalues in the isospectral cells, up to the several percent level, from which on localized structural changes in the eigenstates

are manifest.

Isospectrally patterned lattices open a new pathway of systematically exploring and controlling the localization delocalization transition and designing mobility edges in aperiodic setups even without quasiperiodicity being present. Indeed, there is several ways of generalizing the here studied specific case: one can replace the constant phase gradient by a spatially varying one or an even non-monotonic phase gradient behaviour. Going beyond rotations in two dimensions i.e. shaping the isospectral cells via a 'dynamics' in the higher dimensional angular space represents an interesting and promising avenue to be pursued.

Experimental platforms that might be suited to realize the isospectrally patterned aperiodic lattices could be integrated photonic waveguide lattices [58, 59] or optical lattice/tweezer-based ultracold atomic systems which offer an astounding control of both external as well internal atomic degrees of freedom [60, 61].

This work has been supported by the Cluster of Excellence "Advanced Imaging of Matter" of the Deutsche Forschungsgemeinschaft (DFG)-EXC 2056, Project ID No. 390715994. P.S. acknowledges the unique atmosphere and scientific discussions at ITAMP, Cambridge, in the framework of an extended scientific visit. P.S. thanks M. Röntgen for helpful discussions and Th. Posske for a careful reading of the manuscript as well as fruitful interactions.

* Peter.Schmelcher@physnet.uni-hamburg.de

- [1] M. Hamermesh, Group Theory and Its Applications to Physical Problems, Dover Books on Physics and Chemistry, 1989.
- [2] N.W. Ashcroft and N.D. Mermin, Solid State Physics, Holt-Saunders, 1976.
- [3] J. Singleton, Band Theory and Electronic Properties of Solids, Oxford Master Series in Condensed Matter Physics, Oxford University Press 2001.
- [4] P.A. Lee and T. V. Ramakrishnan, Disordered electronic systems, Rev.Mod.Phys. 57, 287 (1985).
- [5] T. Brandes, and S. Kettemann, The Anderson Transition and its Ramifications - Localisation, Quantum Interference, and Interactions, Lect.Not.Phys. 630, Berlin: Springer Verlag (2003).
- [6] E. Maciá Barber, Aperiodic Structures in Condensed Matter, Fundamentals and Applications, Series in Condensed Matter Physics, CRC Press 2009.
- [7] E. Maciá-Barber, Quasicrystals, Fundamentals and Applications, CRC Press 2021.
- [8] D. Shechtman, I. Blech, D. Gratias, and J. W. Cahn, Metallic phase with long-range orientational order and no translational symmetry, Phys.Rev.Lett. 53, 1951 (1984).
- [9] J.B. Suck, M. Schreiber, P. Häussler, Quasicrystals: An Introduction to Structure, Physical Properties and Applications, Springer Science & Business Media 2002.

- [10] T. Janssen, Crystallography of quasi-crystals, *Act. Crystall.* A 42, 261 (1986).
- [11] C. Berger, T. Grenet, P. Lindqvist, P. Lanco, J. Grieco, G. Fourcaudot and F. Cyrot-Lackmann, The new AIP-dRe icosahedral phase: Towards universal electronic behaviour for quasicrystals?, *Solid State Commun.* 87, 977 (1993).
- [12] A.P. Vieira, Low-Energy Properties of Aperiodic Quantum Spin Chains, *Phys.Rev.Lett.* 94, 077201 (2005).
- [13] D. Tanese, E. Gurevich, F. Baboux, T. Jacqmin, A. Lemaitre, E. Galopin, I. Sagnes, A. Amo, J. Bloch and E. Akkermans, Fractal Energy Spectrum of a Polariton Gas in a Fibonacci Quasiperiodic Potential, *Phys.Rev.Lett.* 112, 146404 (2014).
- [14] A. Jagannathan, The Fibonacci quasicrystal: Case study of hidden dimensions and multifractality, *Rev.Mod.Phys.* 93, 045001 (2021).
- [15] C. Morfonios, P. Schmelcher, P.A. Kalozoumis and F.K. Diakonou, Local symmetry dynamics in one-dimensional aperiodic lattices: a numerical study, *Nonl.Dyn.* 78, 71 (2014).
- [16] E. de Prunelé and X. Bouju, Fibonacci, Koch and Penrose structures: Spectrum of finite subsystems in three-dimensional space, *Phys.Stat.Sol.(b)* 225, 95 (2001).
- [17] E. de Prunelé, Penrose structures: Gap labeling and geometry, *Phys.Rev.B* 66, 094202 (2002).
- [18] M.A. Bandres, M.C. Rechtsman and M. Segev, Topological photonic quasicrystals: Fractal topological spectrum and protected transport, *Phys.Rev.X* 6, 011016 (2016).
- [19] P. Vignolo, M. Bellec, J. Böhm, A. Camara, J.M. Gambaudou, U. Kuhl and F. Mortessagne, Energy landscape in a Penrose tiling, *Phys.Rev.B* 93, 075141 (2016).
- [20] E. Maciá, Clustering resonance effects in the electronic energy spectrum of tridiagonal Fibonacci quasicrystals, *Phys.Stat.Sol.B* 254, 1700078 (2017).
- [21] N. Mott, The mobility edge since 1967, *J.Phys. C: Solid State Physics*, 20, 3075 (1987).
- [22] A. Aubry and G. André, Analyticity breaking and Anderson localization in incommensurate lattices, *Ann.Isr.Phys.Soc.* 3 (133), 18 (1980).
- [23] S. Das Sarma, S. He, and X. C. Xie, Mobility edge in a model one-dimensional potential, *Phys.Rev.Lett.* 61, 2144 (1988).
- [24] S. Das Sarma, S. He, and X. C. Xie, Localization, mobility edges, and metal-insulator transition in a class of one-dimensional slowly varying deterministic potentials, *Phys.Rev. B* 41, 5544 (1990).
- [25] Y. Hashimoto, K. Niizeki, and Y. Okabe, A finite-size scaling analysis of the localization properties of one-dimensional quasiperiodic systems, *J.Phys.A* 25, 5211 (1992).
- [26] J. Biddle, B. Wang, D. J. Priour, and S. Das Sarma, Localization in one-dimensional incommensurate lattices beyond the Aubry-André model, *Phys.Rev.A* 80, 021603(R) (2009).
- [27] J. Biddle and S. Das Sarma, Predicted mobility edges in one-dimensional incommensurate optical lattices: An exactly solvable model of Anderson localization, *Phys.Rev.Lett.* 104, 070601 (2010).
- [28] J. Biddle, D. J. Priour, B. Wang, and S. Das Sarma, Localization in one-dimensional lattices with non-nearest-neighbor hopping: Generalized Anderson and Aubry-André models, *Phys.Rev.B* 83, 075105 (2011).
- [29] S. Ganeshan, J. H. Pixley, and S. Das Sarma, Nearest neighbor tight binding models with an exact mobility edge in one dimension, *Phys.Rev.Lett.* 114, 146601 (2015).
- [30] F. Liu, S. Gosh and Y.D. Chong, Localization and adiabatic pumping in a generalized Aubry-André-Harper model, *Phys.Rev.B* 91, 014108 (2015).
- [31] X. Li, S. Ganeshan, J.H. Pixley and S. Das Sarma, Many-Body Localization and Quantum Nonergodicity in a Model with a Single-Particle Mobility Edge, *Phys.Rev.Lett.* 115, 186601 (2015).
- [32] X. Li, X.P. Li, and S. Das Sarma, Mobility edges in one-dimensional bichromatic incommensurate potentials, *Phys.Rev.B* 96, 085119 (2017).
- [33] C. Monthus, Multifractality in the generalized Aubry-André quasiperiodic localization model with power-law hoppings or power-law Fourier coefficients, *Fractals* 27, 1950007 (2019).
- [34] X. Li and S. Das Sarma, Mobility edge and intermediate phase in one-dimensional incommensurate lattice potentials, *Phys.Rev.B* 101, 064203 (2020).
- [35] S. Roy, T. Mishra, B. Tanatar, and S. Basu, Reentrant localization transition in a quasiperiodic chain, *Phys. Rev. Lett.* 126, 106803 (2021).
- [36] Y. He, S. Xia, D.G. Angelakis, D. Song, Z. Chen and D. Leykam, Persistent homology analysis of a generalized Aubry-André-Harper model, *Phys.Rev.B* 106, 054210 (2022).
- [37] M. Gonçalves, B. Amorim, E. V. Castro, and P. Ribeiro, Hidden dualities in 1D quasiperiodic lattice models, *SciPost Phys.* 13, 046 (2022).
- [38] M. Gonçalves, B. Amorim, E. Castro and P. Ribeiro, Renormalization group theory of one-dimensional quasiperiodic lattice models with commensurate approximants, *Phys.Rev.B* 108, L100201 (2023).
- [39] D. D. Vu and S. Das Sarma, Generic mobility edges in several classes of duality-breaking one-dimensional quasiperiodic potentials, *Phys.Rev.B* 107, 224206 (2023).
- [40] F.A. An, K. Padavič, E.J. Meier, S. Hegde, S. Ganeshan, J.H. Pixley, S. Vishveshwara and B. Gadway, Interactions and Mobility Edges: Observing the Generalized Aubry-André Model, *Phys.Rev.Lett.* 126, 040603 (2021).
- [41] Y. Wang, J.-H. Zhang, Y. Li, J. Wu, W. Liu, F. Mei, Y. Hu, L. Xiao, J. Ma, C. Chin and S. Jia, Observation of Interaction-Induced Mobility Edge in an Atomic Aubry-André Wire, *Phys.Rev.Lett.* 129, 103401 (2022).
- [42] H.P. Lüschen, S. Scherg, T. Kohlert, M. Schreiber, P. Bordia, X. Li, S. Das Sarma, and I. Bloch, Single-Particle Mobility Edge in a One-Dimensional Quasiperiodic Optical Lattice, *Phys.Rev.Lett.* 120, 160404 (2018).
- [43] V. Goblot, A. Strkalj, N. Pernet, J.L. Lado, C. Dorow, A. Lemaitre, L. Le Gratiet, A. Harouri, I. Sagnes, S. Ravets, A. Amo, J. Bloch and O. Zilberberg, Emergence of criticality through a cascade of delocalization transitions in quasiperiodic chains, *Nat.Phys.* 16, 832 (2020).
- [44] F. M. Izrailev and A. A. Krokhnin, Localization and the mobility edge in one-dimensional potentials with correlated disorder, *Phys.Rev.Lett.* 82, 4062 (1999).
- [45] U. Kuhl, F. M. Izrailev, A. A. Krokhnin and H.-J. Stöckmann, Experimental observation of the mobility edge in a waveguide with correlated disorder, *Appl.Phys.Lett.* 77, 633 (2000).
- [46] M. Röntgen, C.V. Morfonios, R. Wang, L. Dal Negro and P. Schmelcher, Local symmetry theory of resonator structures for the real-space control of edge states in binary

- aperiodic chains, *Phys.Rev. B* 99, 214201 (2019).
- [47] P.A. Kalozoumis, C. Morfonios, F.K. Diakonon and P. Schmelcher, Invariant of broken discrete symmetries, *Phys.Rev.Lett.* 113, 050403 (2014).
- [48] P.A. Kalozoumis, C. Morfonios, F.K. Diakonon and P. Schmelcher, Local symmetries in one-dimensional quantum scattering, *Phys.Rev.A* 87, 032113 (2013)
- [49] P.A. Kalozoumis, C. Morfonios, N. Palaiodimopoulos, F.K. Diakonon and P. Schmelcher, Local symmetries and perfect transmission in aperiodic photonic multilayers, *Phys.Rev.A* 88, 033857 (2013).
- [50] C. Morfonios, P.A. Kalozoumis, F.K. Diakonon and P. Schmelcher, Nonlocal discrete continuity and invariant currents in locally symmetric effective Schrödinger arrays, *Ann.Phys.* 385, 623 (2017).
- [51] P. Schmelcher, S. Krönke and F.K. Diakonon, Dynamics of local symmetry correlators for interacting many-particle systems, *J.Chem.Phys.* 146, 044116 (2017).
- [52] V.E. Zambetakis, M.K. Diakonou, P.A. Kalozoumis, F.K. Diakonon, C.V. Morfonios and P. Schmelcher, Invariant current approach to wave propagation in locally symmetric structures, *J.Phys.A* 49, 195304 (2016).
- [53] C.V. Morfonios, M. Röntgen, F.K. Diakonon and P. Schmelcher, Transfer efficiency enhancement and eigenstate properties in locally symmetric disordered finite chains, *Ann.Phys.* 418, 168163 (2020).
- [54] P.A. Kalozoumis, O. Richoux, F. K. Diakonon, G. Theocharis, and P. Schmelcher, Invariant currents in lossy acoustic waveguides with complete local symmetry, *Phys.Rev.B* 92, 014303 (2015).
- [55] N. Schmitt, S. Weimann, C.V. Morfonios, M. Röntgen, M. Heinrich, P. Schmelcher and A. Szameit, Observation of Local Symmetry in Photonic Systems, *Las.Phot.Rev.* 14, 1900222 (2020).
- [56] P. Schmelcher, Degenerate subspace localization and local symmetries, *Phys.Rev.Res.* 6, 023188 (2024).
- [57] Note, that we are using the terminology of a band, for reasons of convenience, although our setup is indeed aperiodic.
- [58] A. Szameit and S. Nolte, Discrete optics in femtosecond-laser-written photonic structures, *J.Phys. B* 43, 163001 (2010).
- [59] M. Kremer, L.J. Maczewsky, M. Heinrich and A. Szameit, Topological effects in integrated photonic waveguide structures, *Opt.Mat.Expr.* 11, 1014 (2021).
- [60] I. Bloch, J. Dalibard, and W. Zwerger, Many-body physics with ultracold gases, *Rev.Mod.Phys.* 80, 885 (2008).
- [61] A. Browaeys and T. Lahaye, Many-body physics with individually controlled Rydberg atoms, *Nat.Phys.* 16, 132 (2020).